Computer Physics Communications 279 (2022) 108460

Contents lists available at ScienceDirect

Computer Physics Communications

www.elsevier.com/locate/cpc

DAMQT 3: Advanced suite for the analysis of molecular density and related properties in large systems ☆,☆☆

Anmol Kumar [a], Rafael López [b,*], Frank Martínez [b], Guillermo Ramírez [b], Ignacio Ema [b], David Zorrilla [c], Sachin D. Yeole [d], Shridhar R. Gadre [e]

[a] School of Pharmacy, University of Maryland, Baltimore 21201, MD, USA
[b] Universidad Autónoma de Madrid, Facultad de Ciencias, Departamento de Química Física Aplicada, Módulo 14, Spain
[c] Universidad de Cádiz, Facultad de Ciencias, Departamento de Química Física, Spain
[d] Department of Chemistry, Bhusawal Arts Science and P. O. Nahata Commerce College, Bhusawal 425201, India
[e] Interdisciplinary School of Scientific Computing, Savitribai Phule Pune University, Pune 411007, India

ARTICLE INFO

Article history:
Received 25 March 2022
Received in revised form 21 June 2022
Accepted 27 June 2022
Available online 8 July 2022

Keywords:
Electron density
Electrostatic potential
Molecular density topology
Sigma-hole
Electrostatics for Intermolecular Complexation
Hellmann-Feynman forces

ABSTRACT

A new version of the DAMQT package specially developed for large systems is reported. The graphical part has been entirely redesigned, using new OpenGL libraries (versions 3.3 or higher) for 3D display. Several 2D plotters and 3D viewers can be launched now in the same session and more than one molecule can be loaded in the same 3D window. Algorithms have been rescaled and modified to work with densities coming from ZDO computations in very big molecular systems (up to thousands of atoms) at a very moderate cost. New functionalities have been added including computation of molecular electrostatic potential over a molecular surface determined as a user-defined density isosurface. The method of Electrostatics for Intermolecular Complexation has been added to the package to serve as an auxiliary tool for cluster geometry optimization. Examples are provided which prove the good performance of the algorithms.

Program summary

Program Title: DAMQT_3
CPC Library link to program files: https://doi.org/10.17632/2rxvgbsnhx.2
Licensing provisions: GPLv3
Programming language: Fortran90, C++ and Python
Supplementary material: Quick-start guide and User's manual in PDF format included in the package. User's manual is also accessible from the GUI.
External routines/libraries: Qt (5.10 or higher), OpenGL (3.3 or higher), ffmpeg (3.4 or higher), OpenBabel (2.3 or higher, optional)
Nature of problem: Analysis and visualization of the molecular electron density, electrostatic potential, critical points, gradient paths, atomic basins, electric field and Hellmann-Feynman forces on nuclei, clusters optimization with EPIC.
Solution method: Molecular electron density is partitioned into (pseudo)atomic fragments by means of the method of Deformed Atoms in Molecules [1]. Electron densities of the fragments are expanded as a series of spherical harmonics times radial factors. The partition is used for defining molecular density deformations and for the fast calculation of several properties associated with density, including electrostatic potential, electric field and Hellmann-Feynman forces over nuclei. Exploration of density and potential topology is facilitated, and the computation of electrostatic potential over an isodensity surface is implemented. Cluster optimization facility with EPIC is also implemented.
Additional comments including restrictions and unusual features: Density matrix must come from an LCAO calculation (any computational level) with spherical (not Cartesian) Slater or Gaussian functions.

☆ The review of this paper was arranged by Prof. N.S. Scott.
☆☆ This paper and its associated computer program are available via the Computer Physics Communications homepage on ScienceDirect (http://www.sciencedirect.com/science/journal/00104655).

* Corresponding author.
E-mail addresses: anmol@outerbanks.umaryland.edu (A. Kumar), rafael.lopez@uam.es (R. López), frankmar98@gmail.com (F. Martínez), guillermo.ramirez@uam.es (G. Ramírez), nacho.ema@uam.es (I. Ema), david.zorrilla@uca.es (D. Zorrilla), sdyeole@basponccollege.org (S.D. Yeole), gadresr007@gmail.com (S.R. Gadre).

https://doi.org/10.1016/j.cpc.2022.108460

The program contains an OPEN statement to binary files (stream) in several files. This statement does not have a standard syntax in Fortran 90. Two possibilities are considered in conditional compilation: Intel's ifort and Fortran2003 standard. This latter is applied to compilers other than ifort (gfortran uses this one, for instance).

References

[1] J. Fernández Rico, R. López, I. Ema, G. Ramírez, J. Mol. Struct., Theochem 727 (2005) 115.

1. Introduction

The reported suite is a thoroughly renewed version of the DAMQT package, aimed as a useful tool for the analysis of molecular electron density (MED) and related properties. The package is based on the partition of MED into pseudo-atomic fragments following the prescription of the Deformed Atoms in Molecules (DAM) method [1,2].

The partition of MED is followed by an expansion of the fragments' densities as a series of radial factors times regular spherical harmonics. Radial factors are numerically computed and piecewise fitted to suitable auxiliary functions. The expansions facilitate the very efficient computation of MED itself, as well as the calculation of related properties like MED deformations, molecular electrostatic potential (MESP), electric field, MED and MESP gradients and hessians, critical points, basins and bonding paths, Hellmann-Feynman forces on nuclei, and MESP sigma-holes [3]. Cluster optimization with Electrostatics for Intermolecular Complexation (EPIC) benefits also from the efficient computation of MESP.

The partition of density accomplished with DAM method retains the image of atoms in molecules as point nuclei surrounded by almost spherical clouds, slightly distorted by the molecular environment, and is an alternative to other partitioning schemes [4–16].

Electron density computed within the LCAO (linear combination of atomic orbitals) framework, can be expressed in terms of densities which are products of the functions of the basis set used in the calculation, $\{\chi_i\}_{i=1}^{m}$:

$$\rho(\mathbf{r}) = \sum_{j=1}^{m}\sum_{k=1}^{m} \rho_{jk}\ \chi_j(\mathbf{r})\ \chi_k(\mathbf{r}) \tag{1}$$

where m stands for the number of basis functions, and ρ_{jk} are the elements of the density matrix in the basis set.

In this work we will consider basis functions consisting of products of radial functions, $\mathcal{R}(r_A)$, either of Gaussian or Slater types, times unnormalized real spherical harmonics, $z_l^m(\theta_A,\phi_A)$:

$$\chi^A_{a,l,m}(\mathbf{r}_A) = \mathcal{R}(r_A)\ z_l^m(\theta_A,\phi_A) \tag{2}$$

The subindex a labels the functions at center A and $\mathbf{r}_A \equiv (x_A, y_A, z_A) = (r_A, \theta_A, \phi_A)$ are the coordinates of a point of space with respect to that center, i.e. $\mathbf{r}_A \equiv \mathbf{r} - \mathbf{R}_A = (x - X_A, y - Y_A, z - Z_A)$, $\mathbf{r}$ is the position of a generic point in the molecular frame, and $\mathbf{R}_A$ that of center A also in that frame.

The (unnormalized) real spherical harmonics are defined as:

$$z_l^m(\theta,\phi) = (-1)^m\ P_l^{|m|}(\cos\theta) \begin{cases} \cos m\phi & (m \geq 0) \\ \sin |m|\phi & (m < 0) \end{cases} \tag{3}$$

$P_l^{|m|}(z)$ being the associated Legendre functions (see [17] eq. 8.751.1).

Thus, eq. (1) can be written as:

$$\rho(\mathbf{r}) = \sum_{A=1}^{N}\sum_{a=1}^{m_A}\sum_{a'=1}^{m_A} \rho_{aa'}\ \chi_a(\mathbf{r}_A)\ \chi_{a'}(\mathbf{r}_A) + \sum_{A=1}^{N}\sum_{\substack{B=1\\B\neq A}}^{N}\sum_{a=1}^{m_A}\sum_{b=1}^{m_B} \rho_{ab}\ \chi_a(\mathbf{r}_A)\ \chi_b(\mathbf{r}_B) \tag{4}$$

where N is the number of nuclei, and m_I is the number of basis functions of atom $I(= A, B)$.

DAM partition assigns to each atom A all the one-center charge distributions $\chi_a(\mathbf{r}_A)\ \chi_{a'}(\mathbf{r}_A)$ centered at its nucleus, and part of each two-center distribution $\chi_a(\mathbf{r}_A)\ \chi_b(\mathbf{r}_B)$ involving its basis functions.

Two-center distributions:

$$\chi_a^A(\mathbf{r}_A)\ \chi_b^B(\mathbf{r}_B) = d^A_{ab}(\mathbf{r}_A) + d^B_{ab}(\mathbf{r}_B) \tag{5}$$

are partitioned following a criterion based on the fast convergence of the long-range expansion of the potential generated by the fragments d^A_{ab}, d^B_{ab} towards that of the full distribution $\chi_a^A\ \chi_b^B$ [18,19].

Since the theoretical foundation of the method is essentially the same as that reported in the previous versions of the package [20,21], here we will just outline the mathematical aspects. Details of the mathematical developments and technical aspects have been thoroughly collected in ref [22], and can be consulted therein.

DAM partition allows us to write the molecular electron density as a sum of pseudo-atomic contributions:

$$\rho(\mathbf{r}) = \sum_A \rho^A(\mathbf{r}_A) \tag{6}$$

with the atomic fragments, ρ^A, given by:

$$\rho^A(\mathbf{r}_A) = \sum_a\sum_{a'} \rho_{aa'}\ \chi_a(\mathbf{r}_A)\ \chi_{a'}(\mathbf{r}_A) + 2\sum_{B\neq A}\sum_a\sum_b \rho_{ab}\ d^A_{ab}(\mathbf{r}_A) \tag{7}$$

These fragments are further expanded in spherical harmonics times radial factors:

$$\rho^A(\mathbf{r}_A) = \sum_{l=0}^{\infty}\sum_{m=-l}^{l} z_l^m(\mathbf{r}_A)\ \rho^A_{lm}(r_A) \tag{8}$$

$z_l^m(\mathbf{r})$ being the unnormalized spherical harmonics of the *regular solid*:

$$z_l^m(\mathbf{r}) = r^l\ z_l^m(\theta,\phi) \tag{9}$$

The infinite sum on l will be actually truncated to a suitable order, l_{max}, what implies an approximation to the exact value.

The radial factors, $\rho^A_{lm}(r)$, are piecewise fitted to products of exponentials times Chebyshev T polynomials (see [17] sec. 8.94):

$$\rho^{A}_{lm}(r_A) \approx e^{-\xi_i r_A} \sum_{k=0}^{n_i} c_k^{(i)}(l,m)\, T_k(t) \tag{10}$$

in a set of intervals, $\lambda_{i-1} \le r_A \le \lambda_i$; $i = 1, \ldots n$, of the variable t:

$$t \equiv 2\,\frac{r_A - \lambda_{i-1}}{\lambda_i - \lambda_{i-1}} - 1 \tag{11}$$

As it has been shown previously, the efficient computation of MED and MESP, and their derivatives as well, is noticeably facilitated by DAM partition/expansion scheme [23,22].

2. MESP sigma hole on a MED isosurface

A feature added to this new release of DAMQT is the efficient computation of MESP on a MED isosurface, usually taken as an approximation to the loose concept of molecular surface. The analysis of this property [24] has revealed a fertile field in the theoretical interpretation of intermolecular bonding [25–29] and reactivity [30], either in terms of *sigma* and *pi* holes introduced by Clark et al. [31–33], or beyond as claimed by Zhang et al. [34].

Furthermore, statistics derived from MESP on the (pseudo) molecular surface have proved to be a very valuable tool for the investigation of the relationships between molecular structure and physicochemical properties [35–39] and successful correlations between these properties and statistical parameters have been found for different families of compounds [40,41]. The new version of the package also implements the computation of these statistics.

Histograms of MESP on the surface are computed, providing a means to characterize molecular behavior in a similar way as COSMO-RS *sigma* profile does [42] and, likewise, properties as molecular polar character or hydrogen bonding behavior can be inferred also from these histograms. Furthermore, contributions to extrema values of MESP on surface are splitted when coming from different molecular regions, to distinguish those cases in which a single region of the molecule is responsible for the hydrogen bond donor (or acceptor) character, from those in which several regions contribute to it.

These histograms are expected to be useful as a possible aid in pre-screening or screening processes in molecular engineering and drug design [43,44], an alternative complementary to other MESP-based techniques for the analysis of molecular similarity [45–47] and molecular recognition [48].

Spectrographs of MESP values in MED isosurface can be displayed in the 3D viewer, together with their local 2D critical points. MESP histograms can be displayed in the new 2D plotter.

3. EPIC for cluster building

The most valuable novelty in the package regarding applications is the facility for cluster optimization. This release of DAMQT implements Electrostatics for Intermolecular Complexation (EPIC) [49–53] model for rapid geometry optimization of non-covalently interacting large molecular systems. Quantum chemical optimization of large molecular systems such as molecular clusters and weakly interacting molecular complexes, becomes increasingly time consuming because of the high scaling of the methods involved, poor convergence and large number of closely spaced local minima in their potential energy surface. EPIC model allows rapid geometry optimization of weakly interacting systems by minimizing the potential energy of guest system in the presence of MESP of the host system. The methodology employed in the original EPIC model [49,53] required MESP of the host system on a grid along with MESP critical points (CPs). The MESP CPs were used as a guide for optimal placement of the guest system. For building energetically favorable structures, the positively charged atom/s of the guest system was/were placed near the deep negative-valued minima i.e. $(3,+3)$ CP in the MESP of the host system. The optimization routine rotated and translated the molecule in all possible directions to find the orientation of the complex with maximum electrostatic interaction. Intersection of van der Waals (vdW) surfaces of the monomeric units was avoided during optimization. This model has been successfully used for building and optimizing DNA base-pairs and trimers [51,52], understanding molecular hydration process [54], hydration of DNA base-pairs [55], and optimizing non-covalently bonded molecular clusters such as $(ZnS)_n$, $(C_6H_6)_n$, $(H_2O)_n$ [56], and $(Ag)_n$ [57] clusters. Despite successful application of this EPIC model, the actual work-flow was a combination of discrete calculations and involved use of at least three different softwares *i.e.* a QM engine, EPIC optimizer and a molecular visualizer with molecular editing capabilities.

The current features of DAMQT provide a hotbed for complete integration of EPIC model with enhanced efficiency, usability and broader applicability. The 3D viewer now allows us placement of guest system near the host in presence or absence of MESP CPs of the latter. Geometric parameters (distances, angles and dihedrals) can be displayed on the canvas to assist the build up of the starting structure. The new EPIC module integrated herein also allows automated placement of guest system by utilizing its partial charge distribution and the topological information of the host system. The ease of building good initial molecular arrangement reduces the manual effort and accelerates the optimization process. To further simplify the functioning of EPIC optimizer, use of MESP-derived point charges of guest system is made optional. User-defined charges can be supplied in a file containing atoms names in one column and corresponding partial charges in the following column. In the case of building a homo-dimer, partial charges of the guest molecule can also be obtained from .mltmod file containing the moduli of the atomic multipole moments (see User and Quick Start Guide for more details) of host molecule, generated by DAMSTO/DAMGTO programs (invoked under Atomic densities tab in DAMQT-GUI). As an auxiliary protocol, the EPIC routine utilizes various charge models available in OpenBabel [58,59] to obtain partial charges [60] on the guest molecule, which can be used for EPIC optimization. This protocol avoids the requirement of any QM-calculation for charge estimation. However, for higher accuracy of optimization procedures, ESP derived charges are better suited [56]. Interaction energy in EPIC is given by

$$E_{EPIC} = \sum_i V_{A,i}, q_{B,i} \tag{12}$$

wherein, $V_{A,i}$ is the MESP value of host molecule at the i^{th} atomic position of the guest molecule, and $q_{B,i}$ is the partial charge on i^{th} atom of the pertaining guest molecule. Ability of DAMQT to provide MESP value and related gradients at any given point eliminates the need of pre-calculated MESP grid data, thus making the algorithm considerably faster. Rapid mapping of MESP and its critical points along with parallel computing capabilities of DAMQT removes all hurdles in the usability of EPIC optimizer and facilitates its application to large and relevant systems.

EPIC optimization starts with rotation of guest geometry to find its most energetically favorable orientation in the electric field of host molecule. This is followed by single translation step in the direction of net electrostatic force acting on the guest molecule. The step-size used for translation is scaled by the normalized component of the net force-vector. After each translation step, a rotation step is performed to obtain optimal orientation at the updated position. Consequently, EPIC optimization ends with the rotation step. If more than one guest geometry needs to be optimized, the subsequent geometries are optimized in the presence of both QM-derived ESP of host molecule and point-charge-derived ESP of all

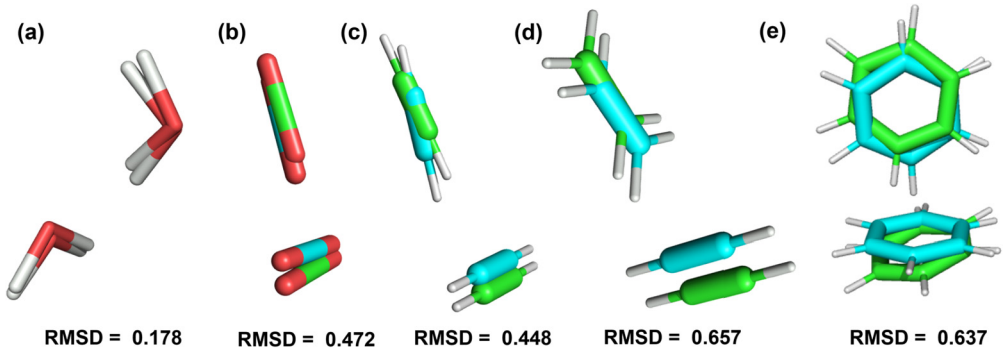

Fig. 1. Comparison between EPIC optimized geometries and QM optimized geometries (denoted by C atoms in blue and green, respectively) for five dimers (a) H_2O-dimer, (b) CO_2-dimer, (c) C_2H_2-dimer, (d) C_2H_4-C_2H_2, (e) C_6H_6-dimer. RMSD scores obtained between the two geometries are also shown. See text for more details. (For interpretation of the colors in the figure(s), the reader is referred to the web version of this article.)

the previously added guest molecules. During each optimization step, scaled vdW radii of the atoms (default scaling factor = 0.7) are used to check if molecular vdW surfaces are intersecting each other. The final geometry obtained after each rotation or translation step is saved in a trajectory file. After optimization of guest geometry, the trajectory file can be used to develop animation of EPIC optimization process. The animation builder utilizes quaternion interpolation to create smoother transition between the geometries saved in the trajectory file. The animation can also be recorded and played back on the canvas, as shown in the movie included in the supplementary material. If the end goal is to obtain QM optimized geometry of the complex, DAMQT now provides a QM input writer for various different QM packages (Gaussian, Gamess, Molpro, Mopac, Nwchem, Psi4) which automatically utilizes coordinates of EPIC optimized geometry as starting point for QM optimization. If the above mentioned QM engines are installed on the same machine which is used to launch DAMQT session, the QM calculation can be directly executed from DAMQT-GUI. This feature greatly reduces the time consumed in building and growing energetically favorable molecular clusters. Furthermore, DAMQT also prepares the job submission scripts for some of the popular job schedulers viz. SLURM, PBE and SGE to facilitate the QM calculation on available HPC facility.

It must be recalled that, if the output of the QM calculation is to be used for the density analysis with DAMQT, the calculation must be done using basis functions with spherical harmonics (not Cartesian). This is taken into account in the input files generated with the templates by including the pertaining option when required.

We demonstrate the use of EPIC module integrated in DAMQT 3 for building few molecular dimers as test-case. QM optimization of the host molecule was performed at MP2/aug-cc-pvDZ level of theory in Gaussian09 program. The atomic expansion of density with multipolar expansion ($l = 15$) was derived from the formatted checkpoint file and was saved into *damqt* and *dmqtv* files. The optimized coordinates of the host molecule was projected on the 3D viewer canvas along with coordinates of the guest molecule using "Add molecule" button. The guest molecule was then shifted near the host system using mouse clicks and keyboard shortcuts (see User and Quick Start Guide for more details). EPIC optimization was initiated using "Optimize cluster" button which considers first molecule with associated *damqt* file as the host and the following molecules as guests. User can change this default consideration. After EPIC optimization, "Quantum Mechanics" button was used to generate Gaussian09 input files for QM optimization of cluster geometries at MP2/aug-cc-pvDZ level of theory and basis-set, with the `5D, 7F` option for spherical basis set. Ultimately, QM optimized geometries were compared to the EPIC optimized geometries. The reliability of EPIC method is exemplified by small root mean square deviation (RMSD) between Cartesian coordinates of EPIC and QM optimized geometries (see Fig. 1) for different types of molecular systems. RMSD is calculated as the square root of the mean of the square of the distances between the atoms with same index in the two supplied structures. Water dimer shows smallest difference between EPIC and QM optimized geometry (RMSD = 0.178). Obtaining correct orientation and intermolecular distance of water dimer is of special significance because of the tetrahedral distribution of electronic charge around water molecule. CO_2-dimer, C_2H_2-dimer and C_6H_6-dimer also show high resemblance between EPIC and QM optimized geometries. The molecular interaction between C_2H_4 and C_2H_2 hetero-dimer is also well-represented. The close resemblance of EPIC optimized geometry with their QM analogs emphasizes the use of EPIC model for reliably generating molecular clusters of larger size.

4. Changes in 2D plotter and 3D viewer

Improvements in DAMQT 3 also include the entirely new implementations of 2D plotter and 3D viewer in the Graphical User Interface (GUI) – see Fig. 2. Now, several 2D plots and 3D displays can be opened in a session. They are deployed outside the GUI's main window, and each 2D plotter or 3D display has its own menu attached to the viewer. These menus can be undocked to increase the width of the canvas.

Many new functionalities have been added in both cases. Thus, 2D plotter allows us to load and display different types of figures together (i.e. isosurfaces, field lines and critical points), and a new type of plot for histograms of MESP on a density isosurface has been included.

In case of 3D viewer, changes are even more significant. Now, more than one molecule can be loaded in the same canvas, and functionalities are implemented to handle single molecules as well as the set of loaded molecules as a whole. Geometry parameters (distances, angles and dihedrals) can be now computed and displayed both for single molecules and between molecules. EPIC cluster optimization can be launched from the viewer and the results can be visualized and animated on the canvas. Spectrograms of MESP over an isodensity surface can be visualized, as well as their local 2D critical points.

3D viewer has been implemented using the new OpenGL libraries (versions 3.3 or above) to take full advantage of modern GPUs capabilities. This means that, to visualize the 3D structures, both the system hardware, libraries and drivers must conform this requirement. The lack of a suitable version of any of these components may lead to an error in execution, or just cause that the objects will not be visible. When this happens, it is convenient to look at the standard output where a message with the OpenGL version actually taken is displayed.

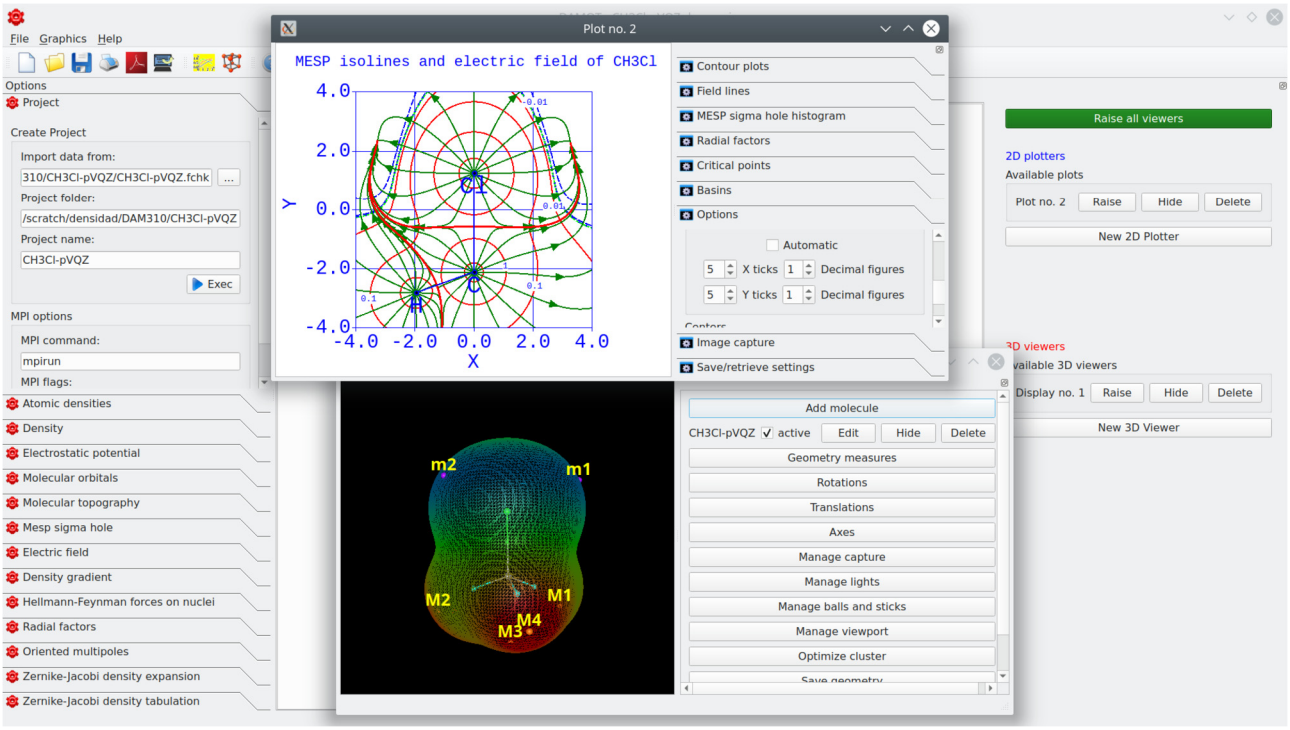

Fig. 2. Graphical User interface, 2D plotters and 3D viewers of DAMQT 3.

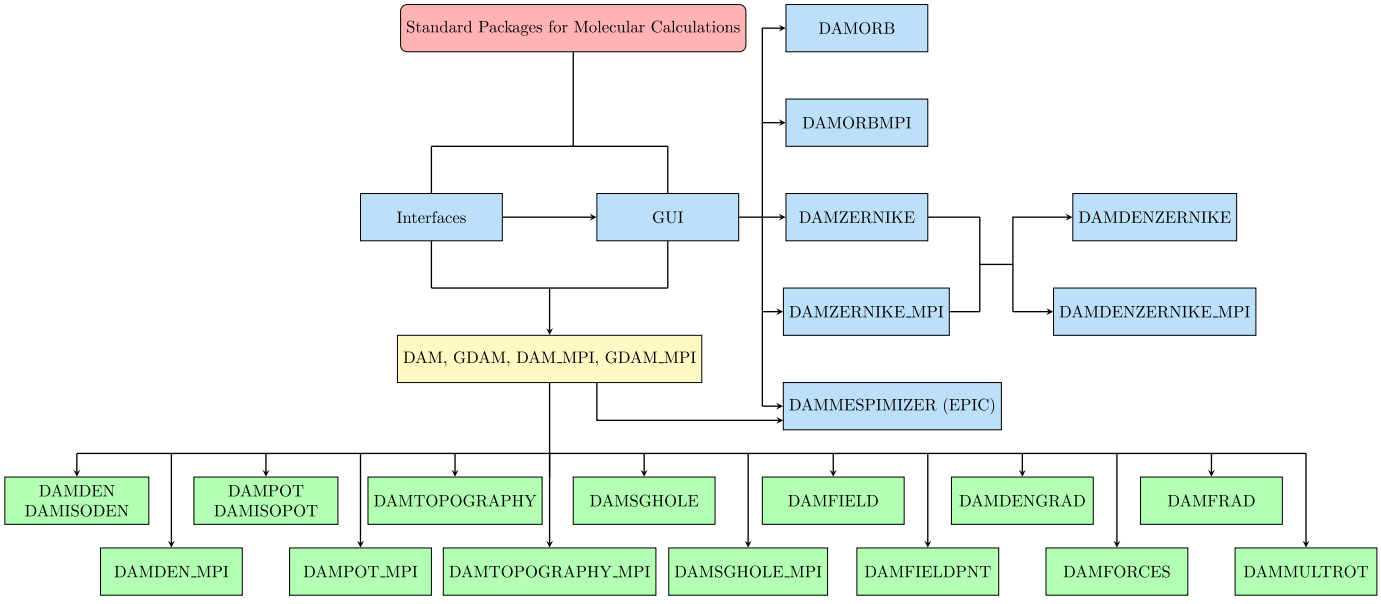

Fig. 3. Structure of DAMQT 3.

The number of 2D plotters and 3D viewers that can be launched in one session is limited only by the system resources.

Declaration of competing interest

The authors declare that they have no known competing financial interests or personal relationships that could have appeared to influence the work reported in this paper.

Data availability

No data was used for the research described in the article.

Appendix A. New structure of the package

DAMQT 3 has the modular structure shown in Fig. 3. The starting point is a molecular calculation with a standard package at any level of calculation (HF, DFT, CI, CAS, MRDCI, ...) within the LCAO framework.

Several interfaces are included in the package to read output files of some popular suites for molecular calculations and create suitable input files for DAMQT. For programs lacking of suitable interfaces, instructions are given in the manual to create these files.

The geometry and basis set file together with the molecular orbitals file are sufficient to compute the values of molecular orbitals

over a 2D or 3D grid by means of DAMORB320 program (or its mpi version DAMORB_mpi320).

To perform DAM analysis of the molecular density, it is necessary to carry out the partition by running the DAMSTO320 module, in case of Slater functions, or DAMGTO320, for Gaussians (DAMSTO320_mpi and DAMGTO320_mpi with mpi). These modules also render charges and multipoles associated to pseudo-atomic fragments.

Once the partition is done, different modules can be accessed to compute MED, MED deformations [61], MESP and electric field (MEF), Hellmann-Feynman forces, radial factors of fragments expansion and locally oriented multipoles. Topology of MED and MESP can be studied by computing CPs, gradient paths and atomic basins. 2D and 3D grids can be generated for all these properties and visualized with the built-in viewers. To accomplish these tasks, the following procedures have been implemented in the package:

- *DAMDEN320*: computation of the density and density deformations for the whole molecule, atomic fragments and functional groups. 2D and 3D grids can be generated for plotting and visualization with DAMQT 3 built-in viewers. Gradient, laplacian and second derivatives can be also (optionally) computed.
- *DAMDENGRAD320*: computation of MED gradient lines.
- *DAMISODEN320*: computation of MED isosurfaces and their normals.
- *DAMPOT320*: computation of the electrostatic potential including 2D and 3D grid generation. Same comments as in DAMDEN320 also hold here.
- *DAMISODEN320*: computation of MESP isosurfaces and their normals.
- *DAMTOPO320*: analysis of MED and MESP topology. Computation of critical points (CPs), hessian eigenvectors and eigenvalues at CPs, gradient path and atomic basins is carried out using DAM partition/expansion.
- *DAMFIELD320*: fast computation of electric field lines including file generation for 3D plotting.
- *DAMFIELDPNT320*: computation of electric field lines on user-defined sets of points.
- *DAMFORCES320*: Hellmann-Feynman forces on nuclei.
- *DAMFRAD320*: tabulation of radial factors and their first and second derivatives.
- *DAMMULTROT320*: tabulation of atomic multipolar moments in a locally oriented frame.
- *DAMORB320*: 2D and 3D grid computation for molecular orbitals.
- *DAMSGHOLE320*: computation of MESP on a MED isosurface.
- *DAMZERNIKE320*: computation of one-center MED expansion in a ball in terms of Canterakis-Zerkine or Jacobi functions.
- *DAMMESPIMIZER320*: cluster optimization with EPIC.

All these programs can be run directly from the Graphical User Interface (GUI) – see Fig. 2 – or, alternatively, as commands on a console terminal or in batch. In these cases, the GUI can be used to generate suitable input files. Parallel versions with mpi are also included for the most time-consuming programs.

Interfaces can be run either from the GUI outside. Running from the GUI only requires double clicking on a suitable file. A quick-start guide and a user manual, both in PDF format, are included in the package. The manual can be also accessed with the help key in the GUI.

An updated version of the package can be downloaded freely from: https://github.com/chemtopotools/DAMQT.git.

Appendix B. Supplementary material

Supplementary material related to this article can be found online at https://doi.org/10.1016/j.cpc.2022.108460.

References

[1] J.F. Rico, R. López, I. Ema, G. Ramírez, E. Ludeña, J. Comput. Chem. 25 (2004) 1355.
[2] J.F. Rico, R. López, I. Ema, G. Ramírez, J. Mol. Struct., Theochem 727 (2005) 115.
[3] P. Politzer, J.S. Murray, Crystals 9 (2019) 165.
[4] R.F. Stewart, E.R. Davidson, W.T. Simpson, J. Chem. Phys. 42 (1965) 3175.
[5] A. Mazziotti, R.G. Parr, G. Simons, J. Chem. Phys. 59 (1973) 939.
[6] F.L. Hirshfeld, Theor. Chim. Acta 44 (1977) 129.
[7] R.F. Stewart, Isr. J. Chem. 16 (1965) 124.
[8] R.F.W. Bader, T.T. Nguyen-Dang, Adv. Quantum Chem. 14 (1981) 63.
[9] A. Becke, R. Dickson, J. Chem. Phys. 89 (1988) 2993.
[10] B. Delley, J. Chem. Phys. 92 (1990) 508.
[11] F.M. Bickelhaupt, N.J.R. van Eikema Hommes, C.F. Guerra, E.J. Baerends, Organometallics 15 (1996) 2923.
[12] D.S. Kosov, P.L.A. Popelier, J. Chem. Phys. 113 (2000) 3969.
[13] C.F. Guerra, J.W. Handgraaf, E.J. Baerends, F.M. Bickelhaupt, J. Comput. Chem. 25 (2004) 189.
[14] A.T.B. Gilbert, P.M.W. Gill, S.W. Taylor, J. Chem. Phys. 120 (2004) 7887.
[15] D. Vanfleteren, D. Van Neck, P. Bultinck, P. Ayers, M. Waroquier, J. Chem. Phys. 132 (2010) 164111.
[16] M. Franchini, P.H.T. Philipsen, E. van Lenthe, L. Visscher, J. Chem. Theory Comput. 10 (2014) 1994.
[17] I.S. Gradshteyn, I.M. Ryzhik, Table of Integrals, Series and Products, 4th edn., Academic Press, New York, 1980.
[18] J.F. Rico, R. López, G. Ramírez, J. Chem. Phys. 110 (1999) 4213.
[19] J.F. Rico, R. López, I. Ema, G. Ramírez, J. Chem. Phys. 117 (2002) 533.
[20] R. López, J.F. Rico, G. Ramírez, I. Ema, D. Zorrilla, Comput. Phys. Commun. 180 (2009) 1654.
[21] R. López, J.F. Rico, G. Ramírez, I. Ema, D. Zorrilla, Comput. Phys. Commun. 192 (2015) 289.
[22] R. Lopez, F. Martinez, I. Ema, J.M. Garcia de la Vega, G. Ramirez, Computation 7 (2019) 64.
[23] J.F. Rico, R. López, I. Ema, G. Ramírez, J. Comput. Chem. 25 (2004) 1347.
[24] F.A. Bulat, A. Toro-Labbé, T. Brinck, J.S. Murray, P. Politzer, J. Mol. Model. 16 (2010) 1679.
[25] Q.Z. Li, R. Li, P. Guo, H. Li, W.Z. Li, J.B. Cheng, Comput. Theor. Chem. 980 (2012) 56.
[26] X. Guo, Y.W. Liu, Q.Z. Li, W.Z. Li, J.B. Cheng, Chem. Phys. Lett. 620 (2015) 7.
[27] J.E. Del Bene, I. Alkorta, J. Elguero, Mol. Phys. 117 (2019) 1117.
[28] J.M. Oliva-Enrich, I. Alkorta, J. Elguero, Molecules 25 (2020) 1042.
[29] I. Alkorta, J. Elguero, J.M. Oliva-Enrich, Struct. Chem. 31 (2020) 1273.
[30] J.Y. Lim, P.D. Beer, Chemistry 4 (2018) 731.
[31] T. Clark, M. Hennemann, J. Murray, P. Politzer, J. Mol. Model. 13 (2007) 291.
[32] J.S. Murray, P. Lane, T. Clark, P. Politzer, J. Mol. Model. 13 (2007) 1033.
[33] J.S. Murray, P. Lane, P. Politzer, J. Mol. Model. 15 (2009) 723.
[34] Y. Zhang, D. Wang, W. Wang, Comput. Theor. Chem. 1128 (2018) 56.
[35] P. Politzer, P. Lane, J.S. Murray, T. Brink, J. Phys. Chem. 96 (1992) 7938.
[36] J.S. Murray, P. Lane, T. Brinck, P. Politzer, J. Phys. Chem. 97 (1993) 5144.
[37] J.S. Murray, P. Lane, T. Brinck, K. Paulsen, M.E. Grice, P. Politzer, J. Phys. Chem. 97 (1993) 9369.
[38] J.S. Murray, P. Politzer, J. Mol. Struct., Theochem 425 (1998) 107.
[39] J.S. Murray, Z. Peralta-Inga, P. Politzer, K. Ekanayake, P. Lebreton, Int. J. Quant. Chem. 83 (2001) 245–254.
[40] J.S. Murray, K. Paulsen, P. Politzer, Proc. Indian Acad. Sci. 106 (1994) 267.
[41] J.S. Murray, T. Brink, P. Lane, K. Paulsen, P. Politzer, J. Mol. Struct., Theochem 307 (1994) 55.
[42] A. Klamt, COSMO-RS from Quantum Chemistry to Fluid Phase Thermodynamics and Drug Design, Elsevier, Amsterdam, 2005.
[43] P. Dean, Molecular Similarity in Drug Design, Springer, Oxford (UK), 1995.
[44] A. Kumar, K.Y.J. Zhang, Front. Chem. 6 (2018) 315.
[45] J. Petke, J. Comput. Chem. 14 (1993) 928.
[46] N. Sadlej-Sosnowska, J. Phys. Chem. A 111 (2007) 11134.
[47] R. Carbó-Dorca, P. Mezey, Fundamentals of Molecular Similarity, Mathematical and Computational Chemistry, Springer US, 2013.
[48] D.K. Roy, P. Balanarayan, S.R. Gadre, J. Chem. Sci. 121 (2009) 815.
[49] S.R. Gadre, C. Koelmel, I.H. Shrivastava, Inorg. Chem. 31 (1992) 2279.
[50] S.R. Gadre, P.K. Bhadane, S.S. Pundlik, S.S. Pingale, in: J. Murray, K.D. Sen (Eds.), Molecular Electrostatic Potential: Concepts and Applications, Elsevier, Amsterdam, 1996, pp. 219–522, Chapter 5.
[51] S.R. Gadre, S.S. Pundlik, J. Phys. Chem. B 101 (1997) 3298.
[52] S.R. Gadre, S.S. Pundlik, J. Phys. Chem. B 101 (1997) 9657.
[53] S.R. Gadre, R.N. Shirsat, Electrostatics of Atoms and Molecules, Universities Press, Hyderabad, 2000.

[54] S.S. Pingale, S.R. Gadre, L.J. Bartolotti, J. Phys. Chem. A 102 (1998) 9987.
[55] D. Sivanesan, K. Babu, S.R. Gadre, V. Subramanian, T. Ramasami, J. Phys. Chem. A 104 (2000) 10887.
[56] S.D. Yeole, S.R. Gadre, J. Chem. Phys. 134 (2011) 084111.
[57] P. Ahuja, M. Molayem, S.R. Gadre, J. Phys. Chem. A 123 (2019) 7872.
[58] N.M. O'Boyle, M. Banck, C.A. James, C. Morley, T. Vandermeersch, G.R. Hutchison, J. Chem. Inf. 3 (2011) 33.
[59] The Open Babel Package, version 2.3.1, http://openbabel.org.
[60] J. Gasteiger, M. Marsili, Tetrahedron Lett. 19 (1978) 3181.
[61] J.F. Rico, R. López, I. Ema, G. Ramírez, J. Chem. Theory Comput. 1 (2005) 1083.